Numerical Model on Frost Height of Round Plate Fin Used for Outdoor Heat Exchanger of Mobile Electric Heat Pumps

Moo-Yeon Lee

Department of Mechanical Engineering, Dong-A University, 37 Nakdong-Daero 550beon-gil saha-gu, Busan, Republic of Korea; E-Mail: mylee@dau.ac.kr

Abstract: The objective of this study is to provide the numerical model for prediction of the frost growth of the round plate fin for the purpose of using as a round plate fin-tube heat exchanger (evaporator) under frosting conditions. In this study, numerical model was considering the frost density change with time, and it showed better agreement with experimental data of Sahin (1994) than that of the Kim model (2004) and the Jonse and Parker model (1975). This is because the prediction on the frost height with time was improved by using the frost thermal conductivity reflecting the void fraction and density of ice crystal with frost growth. Therefore, the developed numerical model could be used for frosting performance prediction of the round plate fin-tube heat exchanger.

Keywords: Frost; Height; Round plate fin; Growth

Nomenclature

A	surface area (m^2)
A_c	area of frost column (m^2)
A_a	area of air (m^2)
D	thermal diffusivity in air (m^2/s)
D_h	hydraulic diameter (mm) ($D_h = 4A_c L/A$)
D_o	tube diameter (m)
G	mass flux (kg/m^2 s)
h	heat transfer coefficient (W/m^2 K)
h_m	mass transfer coefficient (kg/m^2 s)
h_h	heat transfer coefficient of frost layer (W/m^2 K)
h_{fc}	enthalpy of the frost crystal (kJ/kg)

h_a air enthalpy (kJ/kg)

h_{a_s} saturated air enthalpy of the frost layer inside (kJ/kg)

Δh latent heat of vapor (kJ/kg)

k_a thermal conductivity of the air (W/m K)

k_{fc} thermal conductivity of the frost column (W/m K)

k_f thermal conductivity of the frost layer (W/m K)

L core depth or appropriate characteristic length (mm)

$\dot{m}$ mass flux (kg/m^2 s)

P_{atm} atmospheric pressure (kPa)

P_o partial pressure of the water vapor at $T_o = 273.15K$ (kPa)

Pr Prandtl number

Re Reynolds number based on the tube diameter (GD_o/μ)

R gas constant (J/Kg K)

Sc Schmidt number ($\frac{\mu}{\rho D}$)

T crystal formation temperature (°C)

T_a air temperature (°C)

T_p plate temperature (°C)

T_s surface temperature (°C)

T_w wall temperature (°C)

t time (min)

μ dynamic viscosity coefficient (N s/m^2)

ω_a humidity ratio of the moist air (kg/kg$_a$)

ω_s humidity ratio of the air at the frost surface (kg/kg$_a$)

X_s frost layer height (m)

x length (m)

β volumetric ratio of frost columns considering void fraction

ρ density (kg/m^3)

ρ_f frost layer density (kg/m^3)

ρ_a density of the air (kg/m^3)

ρ_c sublimation density of the frost crystal (kg/m^3)

1. Introduction

Frost formation and growth of the evaporator operated under frosting conditions are very essential phenomena because it acts as an thermal resistance with decreasing the frosting heat transfer performances in many refrigeration system, air conditioning system and heat pump system [1,2]. Especially, numerous experimental and numerical studies on frosting and its growth have been reported for a long time. Padhmanabhan et al.(2011) [3] studied the semi-empirical model to predict the non-uniform frost growth on fin-tube heat exchangers and validated with the experimental data. The considered fin configuration is rectangular type. Hong et al. (2012) [4] studied frost growth on louvered folded fins of micro-channel heat exchangers. They provided several new data for frost growth on louvered fins and experimentally demonstrated the feasibility of the frost mass and frost height measurements. Xia and Jacobi (2004) [5] studied exact solution to steady heat conduction in a two-dimensional slab on a one-dimensional fin for the purpose of application to frosted heat exchangers. They mentioned that the exact solution is useful in gaining physical insights into the problem, and it is simple, accurate, and less costly to use than numerical solutions. Shao *et al.* (2012) [6] showed the comparison of heat pump performance using fin and tube and micro-channel heat exchangers under frosting conditions. Lee et al. (2011) [7] studied the air-side heat transfer characteristics of spirally-coiled circular fin-tube heat exchanger operating under frosting conditions. They suggested the useful heat transfer correlation to predict the frosting heat transfer coefficient of the fin-tube heat exchanger. In summary, frosting including the frost height and growing is a key factor related to the above-mentioned thermal systems because it is a transient phenomena and not easy to predict.

In these days, concerns of frosting performances of the round plate fin-tube heat exchanger in zero emission vehicles that do not use fossil fuels have been also increased because it considers as outdoor heat exchanger of the electric-driven heat pump system for cabin both heating and cooling. Lee et al. (2012) [8] is studied experimentally frost height of round plate fin-tube heat exchangers under cold weather conditions for mobile heat pumps which has relatively large fin pitches. They mentioned that frosting problem is very important in adoption of the heat exchanger used in the electric-driven heat pump system for zero emission

vehicles such as electric vehicles, fuel cell electric vehicles, hybrid electric vehicles, etc. So, the round plate fin-tube heat exchangers with large fin pitches might be used for zero emission. Also, Cho et al. (2012) [9] mentioned that the use of heat pumps instead of a PTC (positive temperature coefficient) heater is more effective for the longer driving ranges of the above-mentioned vehicles. However, there is a limited amount of data available on the frosting and its performance on the round plate fin. Therefore, the various studies for predictions of the frosting performances including frost height and growing are generally necessary for usages of the outdoor heat exchangers (especially, an evaporator) as applications in the zero emission vehicles.

In this respect, this study aims to predict the frosting behavior on round plate fin under cold weather conditions. The predicted result was then compared with the experimental data suggested by Lee et al. (2012). In addition, the predicted data could be effectively used for designing the round plate fin-tube heat exchanger of the electric-driven heat pumps for zero emission vehicles.

2. Numerical model

Figure 1 shows the schematic diagram of the round plate fin used in this study. The heat transfer rate on the frost was divided into the latent and sensible heat transfer as a function of the temperature and humidity ratio difference between the passing air and frost surface on the cold round plate fin. Based on the numerical modeling results of other researcher (Jonse and Parker (1975) [10], Kim (2004) [11]), the heat and mass transfer rate were calculated by equations (1) and (2).

$$q_t = h_h(T_a - T_s) + \dot{m}\Delta h$$
$$h_h(T_a - T_s) + \rho_f \frac{dX_s}{dt}\Delta h + X_s \frac{d\rho_f}{dt}\Delta h = k_f\left(\frac{dT}{dX_s}\right) \quad (1)$$

$$\dot{m} = h_m(\omega_a - \omega_s) = \frac{d}{dt}(X_s \rho_f) = \rho_f \frac{dX_s}{dt} + X_s \frac{d\rho_f}{dt} \quad (2)$$

However, they calculated with an assumption of a constant frost density on the frost with time. This assumption is unrealistic because the process of the frost growth on the cold plate was a very slow but unsteady process. So, it was treated in an unsteady state in this study. The density changes of the frost surface of the newly developed frost layer were considered with time. Namely, whenever a frost was transferred to a new environment, the continued frost growth assumed a new habit characteristic of the new conditions. The frost density of the newly developed frost layer was calculated from equation (3).

$$\rho_f = \beta \times \rho_c + (1-\beta) \times \rho_a \quad (3)$$

In order to reflect the density changes of newly developed frost layer, the sublimation density of ice crystals was expressed like equation (4) as a function of crystal formation temperature, based on the experimental studies of Fukuta et al. (1969) [12] and Miller and Young (1979) [13]. The least squares approximation of the experimental data that is used for frost growth model is performed by Sahin et al. (2000) [14]. This is because the frost layer is assumed to be consisted of the several frost columns.

Frost columns also consist of ice crystals. The conductivity of frost columns (k_{fc}) only is a function of the frost column density (ρ_c).

$$\begin{aligned} \rho_c &= -10429.56+41.574T \qquad 255.15K < T < 273.15K \\ \rho_c &= 180 \qquad\qquad\qquad\qquad T < 255.15K \end{aligned} \tag{4}$$

Volumetric ratio (β) of the frost column considering the void fraction was expressed as functions of plate temperature, air temperature, and humidity ratio of moist air like equation (5) based on the experimental results of Sahin et al. (1994) [15].

$$\beta = -11.8916 + 0.01371T_P + 0.03269T_a - 112.677\,\omega_a \tag{5}$$

Equation (6) calculated the internal energy changes in control volume as the humid air was changed into the frost crystal and a saturated air of the frost layer inside. As the humid air is infiltrated into the frost, a part of the humid air was used for formations of the new frost layer and the rest of humid air was used to increase the densification of the previous frost layer.

$$\left.\frac{dE}{dt}\right)_{sys} = \left(\rho_c A_c h_{fc} + \rho_a A_a h_{a\_s} - (A_c + A_a)\rho_a h_a\right)\frac{dX_s}{dt} \tag{6}$$

Equation (7) indicated the energy transfer rate by the saturated humid air infiltrated into the previous frost layer.

$$\sum_{out}(\dot{m}\times h) = A_a\, X_s\, \frac{d\rho_f}{dt}\, h_{a\_s} \tag{7}$$

Equation (8) suggested by Sander et al. (1974) [16] was used to calculate the thermal conductivity of the frost column.

$$k_{fc} = (1.202\times10^{-3})\ \rho_c^{0.963} \tag{8}$$

The diffusivity of water vapor in air (D) is calculated from equation (9) and thermal conductivity of the air-side can be approximated to equation (10) suggested by Tso et al. (2006) [17] and Pruppacher and Klett (1978) [18].

$$D = 2.19\times10^{-5}\left(\frac{T}{T_0}\right)^{1.81},\ for\, T_0 = 273.15K \tag{9}$$

$$k_a = \left(1.0465 + 0.017T\right)\times10^{-5} \tag{10}$$

Thus, thermal conductivity of the frost layer can be expressed equation (11) suggested by Sahin (2000). The first term is the effect of the diffusion and sublimation of water vapor in the frost layer. This term is apparently a function of temperature, therefore, the contribution of this term to the frost thermal conductivity varies with the location in the frost layer. The second and third terms are the thermal conductivity contributions of the frost column and the moist air around the frost columns, respectively, as mentioned in Sahin (2000).

$$k_f = 0.131\times10^{-6}(1-\beta)\times\frac{\Delta h P_o P_{atm}}{T_0^{1.94}R^2T^{1.06}}\exp\left[\frac{\Delta h}{R}\left(\frac{1}{T_o}-\frac{1}{T}\right)\right]+\beta k_{fc}+(1-\beta)k_a \quad (11)$$

where P_0 is the partial pressure of water vapor at T_0 = 273.15 K.

In order to calculate the heat transfer coefficient of the round plate fin tube heat exchanger, the equation (12) is used because the flow pattern between the fins could be considered as an internal flow [19]. Thus, equation (12) for an internal flow is the modified form of the heat transfer coefficient suggested by Dittus and Boelter (1930) [20] and the mass transfer rate is calculated by equations (13) and (14) [21].

$$h_h = 0.023\frac{k_a}{D_h}\mathrm{Re}^{0.8}\ \mathrm{Pr}^{0.3} \quad (12)$$

$$h_m = 0.023\frac{D}{D_h}\mathrm{Re}^{0.8}\ Sc^{0.3}\rho_a \quad (13)$$

$$\dot{m} = h_m(\omega_a - \omega_s) \quad (14)$$

Figure 1. Numerical model on frost height prediction at a round plate fin and fin-tube heat exchanger. (a) Control volume on the round plate fin. (b) Control volume on fin-tube.

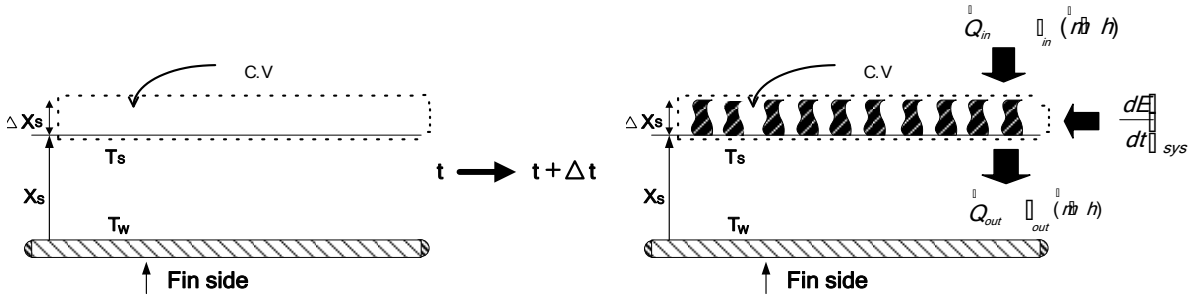

(a) Control volume on round plate fin

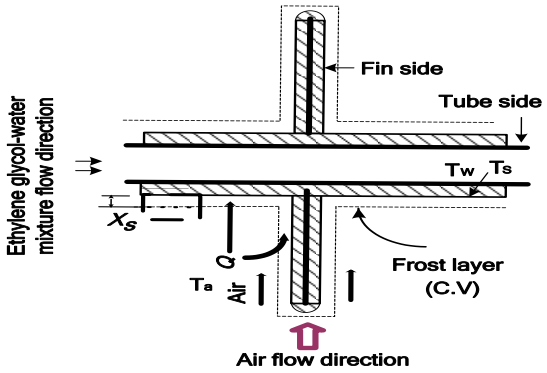

(b) Control volume on round plate fin-tube

Figure 2. Flow diagram of the numerical model.

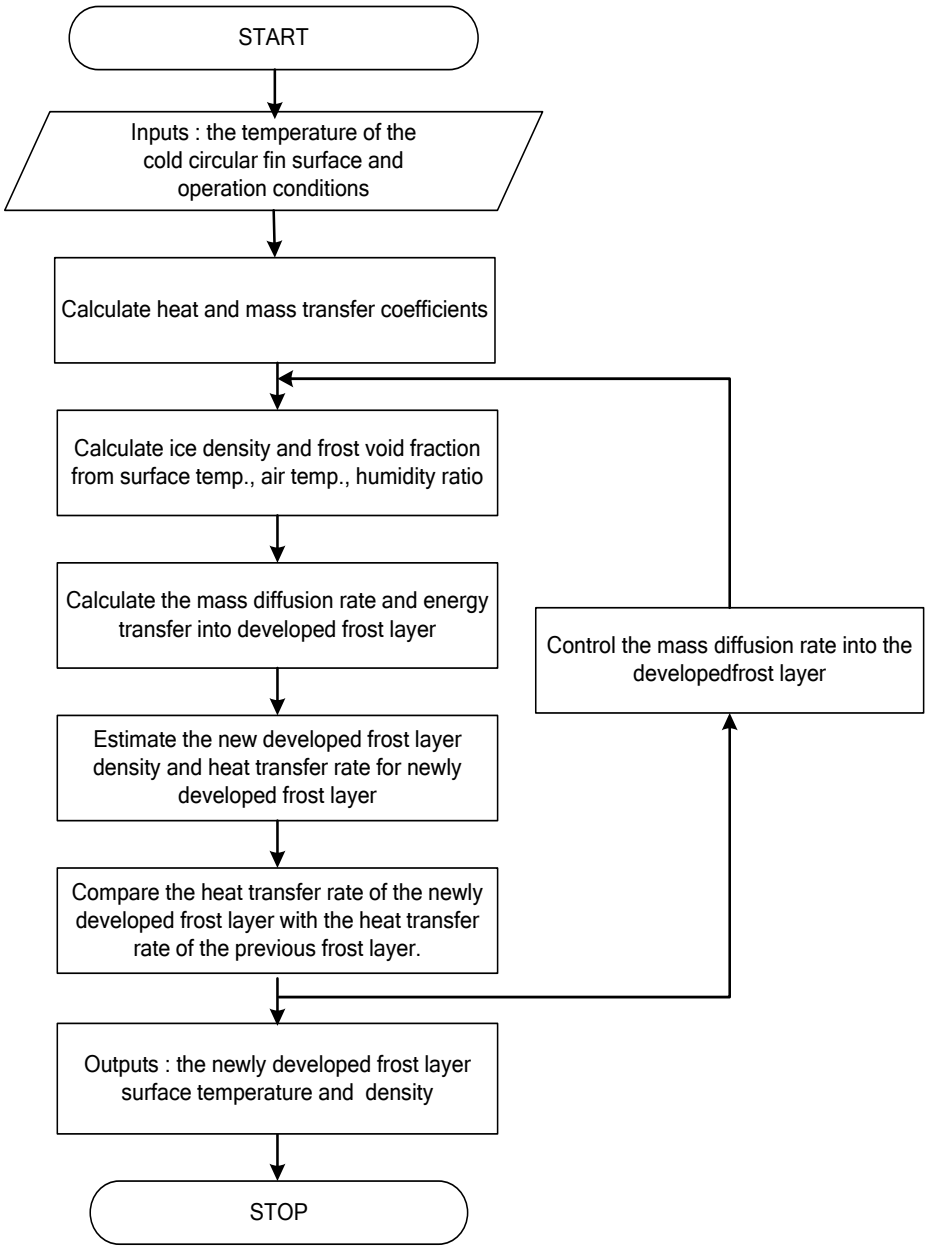

Therefore the heat transfer rate through frost layer and mass transfer rate inside the frost layer were calculated, then surface temperature and density of new developed frost layer were finally calculated. Figure 2 shows the block diagram of the frost growth model in this study. As step 1 was converged with step 2, surface temperature and density of new developed frost layer were calculated.

3. Results and discussion

The developed numerical model reflects the various environmental parameters and unsteady processes of the frost formation and growth. Especially, the density changes of the newly developed

frost layer were considered with time reflecting a new habit characteristic of the new conditions whenever a frost was transferred to a new environment. These points make the present numerical model more realistic than the existing numerical model for prediction of the frost growth.

3.1 Numerical results

The present numerical model on frosting prediction was compared with Jones and Parker model (1975), the experimental data of Sahin (1994), and the Kim model (2004). The present model showed a similar prediction to those of other models for the beginning of the frost formation, but better agreement with the experimental data during the processing of the frost growth with time than the other models. The Jones and Parker model (1975) has been the most commonly used frost growth model until now. However, the Jones and Parker model makes an important assumption to simplify the development of the model: there was assumed to be no spatial variation of frost density even though it varies with time. Accordingly their model did not consider density changes on the frost surface with frost growth. The Kim model (2004) considered the frost thermal conductivity with frost density changes with frost growth. This model made good predictions at the beginning of the frost formation but not so good predictions with as the frost growth progressed. The present numerical model considered the frost thermal conductivity according to the humidity ratio, surface temperature, density change, and void fraction of the frost surface with time. This will be shown to make good predictions for the frost growth.

Figure 3. Comparisons between the present model and other data.

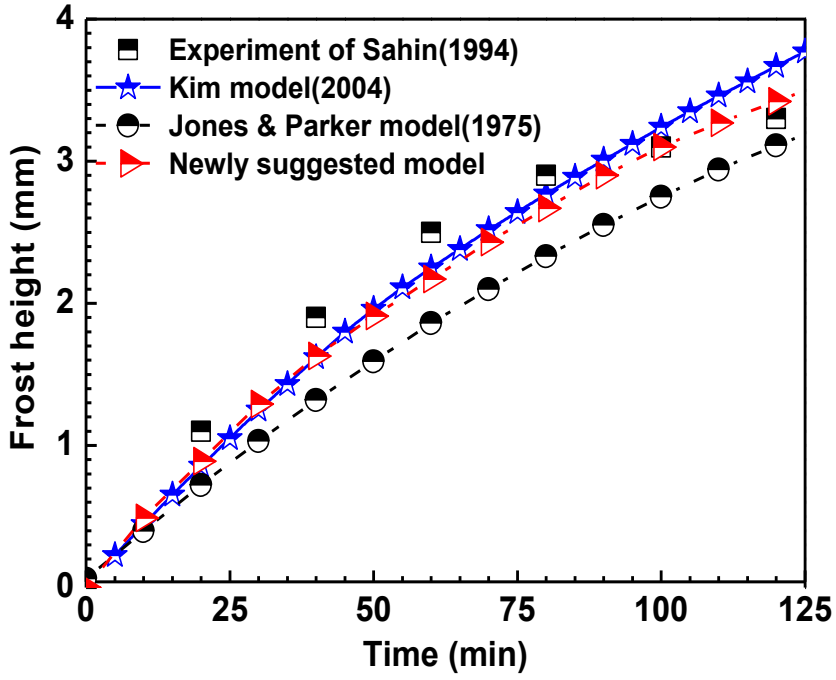

Figure 3 shows the comparisons of the present model with experimental data provided by Sahin (1994), the Jones and Parker model (1975), and the Kim model (2004) under specified conditions with an air temperature of 18.0 ^{o}C, plate temperature of -28.0 ^{o}C, air velocity of 2.1 m/s, and humidity ratio of 0.007 kg/kg$_a$. The newly developed model in this study showed better agreement with the experimental data of Sahin (1994) than the Kim model (2004), which considered the frost thermal conductivity as a function of the frost density, as well as the Jones and Parker model (1975), which assumed the frost density to be constant with time.

Generally, fin configuration and space of the outdoor heat exchanger used in heat pump system for zero emission vehicles such as hybrid electric vehicles, electric vehicles and fuel cell electric vehicles should be simple and large because of the frosting problem and easy defrosting water disposal. So the round plate fin configuration is a good option to adapt as an outdoor heat exchanger for mobile electric heat pumps as mentioned in Lee et al. (2012).

3.2 Validation with experimental data of Lee et al. (2012)

The predicted data using numerical model were compared with the experimental results obtained using a round fin-tube heat exchanger suggested by Lee et al. (2012). Figure 4 shows the comparisons between the numerical data and the experimental data for frost height of the round fin-tube heat exchanger with a fin space of 10.0 mm. It is simulated under an ethylene glycol-water mixture inlet temperature of -15.0 ^{o}C, air flow rate of 1.0 m^3/min, air temperature of 5.0 ^{o}C and relative humidity of 70.0%. The considered fin-tube specifications are expressed in Table 1. Table 1 shows the simulation conditions and specifications of the considered heat exchanger.

Table 1. Conditions and specifications of the considered heat exchanger.

Parameter	Value
Fin space (mm)	10.0
Fin diameter (mm)	23.0
Fin thickness (mm)	0.25
Tube diameter (mm)	8.2
Tube thickness (mm)	0.5
Tube length (mm)	650.0
Materials for a fin and a tube	Aluminum
Inlet air temperature (°C)	5.0
Inlet air relative humidity (%)	70
Airflow rate (m^3/min)	1.0
Inlet temperature of an ethylene glycol-water mixture (°C)	-15.0

The numerical result was validated against the experimental result; both results matched on average to within -3.4%. The numerical data is under-predicted on average 5.8% at first 40 minutes and then over-predicted on average -7.9% after 40 minutes. The frost height predicted from numerical model showed good agreement with the experimental data during at first 40 minutes because the air flow rate was almost unchanged with frost growth. Moreover, the boundary layer interruption between the fins theoretically did not occur until the frost height on the fin surface reached 2.0 mm. However, the agreement between the numerical data and the experimental data after the frost height reached 2.0 mm at 40 minutes showed a slight difference because the numerical model did not consider the boundary layer interruption and pressure drop increase between the fins with frost growth. Based on the theoretical results of the boundary layer analysis using the techniques of Lee (2010) [22] and Mon and Gross (2001) [23], the velocity boundary layer thickness on one side of the fin surface was approximately 3.5 mm at the fin diameter of 23.0 mm with the tube diameter of 8.2 mm. Therefore, boundary layer interruption between fins can occur theoretically for a fin space of 7.0 mm at an air flow rate of 1.0 m^3/min. That is, the boundary layer interruption for a fin space of more than 7.0 mm can be avoided under the given conditions because the boundary layer interruption is largely dependent on the fin space [24].

This is consistent with the results of the Kim (2004) [25]. The error on frost height between experimental data and numerical data is decreased as boundary layer interruption in the fins considered with time. Namely, based on his results, errors between numerical data and experimental data were on average 1.4% with boundary layer interruption but were on average 5.5% without boundary layer interruption. In addition, in our next work, the effects of frost height on boundary layer interruption between the fins with frost growth will be studied because the boundary layer thickness and interruption are important factors in the design of heat exchangers.

Figure 4. Comparison between the experimental data and numerical data with frost growth.

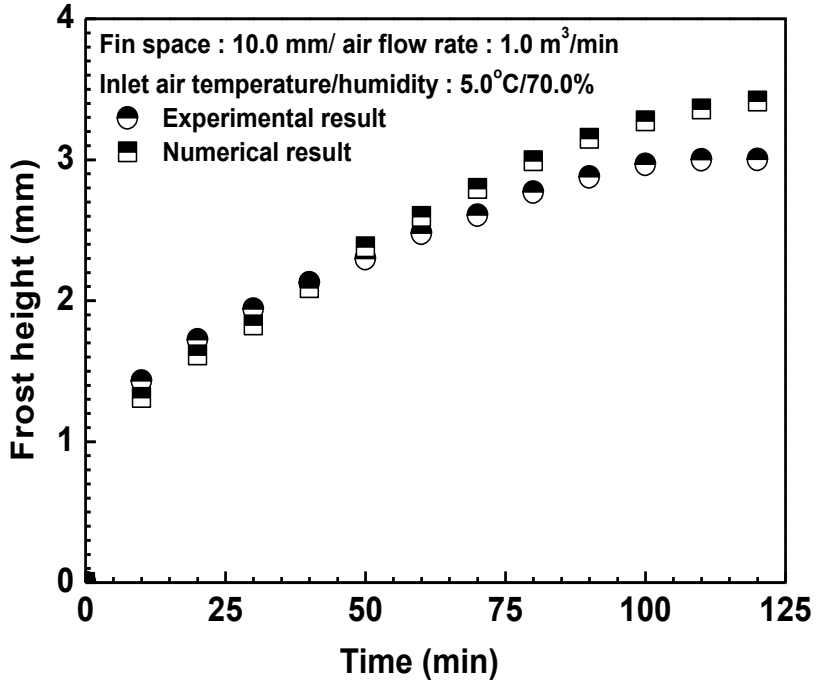

4. Conclusions

The frost height and growing on the round plate fin, which could be used as the outdoor heat exchanger of an electric-driven heat pump in zero emission vehicles were numerically predicted and validated with the published experimental data. The fundamental equation used for the calculation of the heat and mass transfer rate was simple enough to minimize the iteration time. This feature is important when numerical model is used for designing of heat exchangers for low temperature heat pumps under cold weather conditions. The present model showed better predictions than the Jones and Parker model (1975) and the Kim model (2004) for the frost height and growing with time.

(1) The present model developed in this study considered the frost thermal conductivity with the humidity ratio, surface temperature, density change, and void fraction of the frost surface with time.

(2) The frost height for 10.0 mm of fin space showed a similar rate of increase during the 40 minutes because the boundary layer interruption theoretically did not occur for a fin space of during the tests.

(3) The frost height predicted by using the frost growth model showed good agreement with published experiment data suggested by Lee et al. (2012). This is because the prediction of the frost height with time was improved by using an expression for the frost thermal conductivity that reflects the variation of the void fraction and density of ice crystals with the frost growth.

(4) The numerical result was validated against the experimental result; both results matched on average to within -3.4% during the tests.

Acknowledgments

This work was supported by the Dong-A University research fund (2012).

References and Notes

1. Yan, W. M.; Li, H. Y.; Wu, Y. J.; Lin, J. Y.; Chang, W. R.; Performance of finned tube heat exchangers operating under frosting conditions. *Int. J. Heat Mass Transfer*, **2003**, 46, 871-877.
2. Lee, M.; Kang, T.; Kim, Y.; Air-side heat transfer characteristics of spiral-type circular fin-tube heat exchangers. *Int. J. of Refrigeration*, **2010**, 33, 313-320.
3. Padhmanabhan, S. K.; Fisher, D. E.; Cremaschi, L.; Moallem, E.; Modeling non-uniform frost growth on a fin-and-tube heat exchanger. *Int. J. of Refrigeration*, **2011**, 34 (8), 2018-2030.
4. Hong, T.; Cremaschi, L.; Moaellem, E. ; Fisher, D. E.; Measurements of Frost Growth on Louvered Folded Fins of Microchannel Heat Exchangers Part 1: Experimental Methodology. *ASHRAE Transactions*, **2012**, 118 (1), 1101-1115.
5. Xia, Y.; Jacobi, A. M.; An exact solution to steady heat conduction in a two-dimensional slab on a one-dimensional fin: Application to frosted heat exchangers *Int. J. Heat Mass Transfer*, **2004**, 47, 3317-3326.
6. Shao, L. L.; Yang, L.; Zhang, C. L.; Comparison of heat pump performance using fin-and-tube and microchannel heat exchangers under frost conditions. *Applied Energy*, **2010**, 87, 1187–1197.
7. Lee, M. Y.; Kang, T. H.; Joo, Y. J.; Kim. Y. C; Heat transfer characteristics of spirally-coiled circular fin-tube heat exchangers operating under frosting conditions. *Int. J. of Refrigeration*, **2011**, 34, 1, 328-336.
8. Lee M. Y., Kim Y., Lee D. Y. Experimental study on frost height of round plate fin-tube heat exchangers for mobile heat pumps. *Energies*, **2012**, 5(9), 3479-3491.
9. Cho, C. W.; Lee, H. S.; Won, J. P.; Lee, M. Y. Measurement and evaluation of heating performance of heat pump systems using wasted heat from electric devices for an electric bus. *Energies*, **2012**, *5*, 658-669.
10. Jones, B. W.; Parker, J. D.; Frost formation with varying environmental parameters, Journal of Heat Transfer. *Transaction of the ASME*, **1975**, 255-259.
11. Kim, Y. H.; Study on the frosting and defrosting performance of finned tube heat exchangers, Ph. D. Thesis, Korea University, **2004,** 88-101.
12. Fukuta, N.; Experimental studies on the growth of small ice crystals. *Journal of the Atmospheric Sciences*, **1969**, 26, 521-531.
13. Miller, T. L.; Young, K. C.; A numerical simulation of ice crystal growth from the vapor phase. *Journal of the Atmospheric Sciences*, **1979**, 36, 458-469.
14. Sahin, A. Z.; Effective thermal conductive of frost during crystal growth period. *Int. J. of Heat and Mass Transfer*, **2000**, 43, 539-553.
15. Sahin, A. Z.; An experimental study on the initiation and growth of frost formation on a horizontal plate. *Experimental Heat Transfer: An International Journal*, **1994**, 7, 101-119.
16. Sanders, C. T.; The influence of frost formation and defrosting on the performance of air coolers. Ph. D. Thesis, Delft Technical University, **1974**.

17. Tso, C. P.; Cheng, Y. C.; Lai, A. C.; An improved model for predicting performance of finned tube heat exchanger under cold weather condition with frost height variation along fin. *Applied Thermal Engineering*, **2006**, 26, 111 - 120.
18. Pruppacher, H. R.; Klett, J. D.; Microphysics of clouds and precipitation, Reidel, Dordrecht, **1978**.
19. Kim, Y. H.; Kim, Y.; Heat transfer characteristics of flat plate finned-tube heat exchangers with large fin pitch. Int. J. Refrigeration, 2005, 28, 851-858.
20. Holman, J. P.; Heat transfer. 7th edition, McGraw-Hill, UK, **1992**.
21. Incropera, F. P.; DeWitt, D. P.; Fundamentals of heat and mass transfer, 4th edition, Wiley, New York, **1996**.
22. Lee, M. Y.; Heat and mass transfer characteristics of a spirally-coiled circular fin-tube heat exchanger. Ph. D. Thesis, Korea University, **2010**.
23. Mon, M. S.; Gross, U.; Numerical study of fin-spacing effects in annular-finned tube heat exchangers. *Int. J. Heat Mass Transfer*, **2004**, 47, 1953-1964.
24. Lee, S. H.; L, M. Y.; Won, Y. J.; Kim, Y.; Frost growth characteristics of spirally-coiled circular fin--tube heat exchangers. *Int. J. Heat Mass Transfer*, **2012**, 53, 2655-2661.
25. Kim, Y. H.; Study on the frosting and defrosting performance of finned tube heat exchangers, Ph. D. Thesis, Korea University, **2004**, 102-108.